Production Systems and Information Engineering, Miskolc, Vol. 1. (2003), pp. 29-39

CUTTING FORCE MODELING POSSIBILITIES IN OPENGL BASED MILLING SIMULATORS

KÁROLY NEHÉZ*
Department of Information Engineering, University of Miskolc
H-3515 MISKOLC, Hungary
nehez@ait.iit.uni-miskolc.hu

TIBOR CSÁKI
Department of Machine Tools, University of Miskolc
H-3515 MISKOLC, Hungary
csaki@szgtirix.szgt.uni-miskolc.hu

[Received April and accepted October 2002]

* Production Information Engineering Research Team (PIERT) of the Hungarian Academy of Sciences; Department of Information Engineering of the University of Miskolc

Abstract. In the past years, our research activities were focused on several fields in machining simulation and verification. A new milling simulation method and a software application was developed based on pure OpenGL calculating and rendering techniques [1]. As a next step, we tried to investigate the possibilities and practical applications of cutting force modeling in the simulator. This paper examines the developing possibilities of this new feature and describes methods found in the literature [4-11] to determine the cutting force and helps to calculate average or instantaneous cutting force in each tool motion during milling process using the simplest 'volumetric' and an advanced mechanistic model. Using these methods, feedrate can be adjusted more precisely. Since the tool is modeled with a set of polygons in the simulator, therefore it is easy to approximate the instantaneous contact area between tool and workpiece in each tool motion

Keywords: milling simulation, OpenGL, cutting force calculation

1. Introduction

In the early 20th century, *F.W Taylor* performed experiments for 26 years to create a simple solution for the intricate problem of setting safe and efficient cutting conditions. Despite of the progress in cutting tool technology during the last century it is still not easy to determine the optimum spindle speed and federates for metal removal processes. A direct relationship can be found between the cutting conditions and the economics of the metal removal process. The goal is to obtain the least machining time or machining cost while maintaining the safe cutting conditions and high part quality.

Currently, most machining shops employ the traditional method of constant federate cutting for sculptured surface parts. This can result in significant tolerance deviations. [3] The different machining stages have very different requirements. In case of finishing the main aim to ensure constant tool deflection, resulting better tolerances. In roughing, we try to reduce breaking strength of the tool shank, note that in roughing the removable volume is larger than in case of finishing.

2. Calculation models

As it was mentioned in the abstract, there are number of different approaches for optimization and calculation of cutting conditions. In this paper, the most important methods will be showed: volumetric and mechanistic models. Simulators of commercial CAD/CAM systems support geometrical simulation and verification only.

Simulators with cutting force determination capability should answer the following questions:

- Does the local tool stress exceed the strength of the cutter material?
- Can the machine tool supply enough power to cut the workpiece?
- How much is the maximum bending of the current cutting tool?

Other requirement:

- The algorithm should be very efficient and quick. Note that SSM (sculptured surface machining) data files (e.g. CLData) often consist of thousand of tool motions and we must examine the cutting force for each tool step.

2.1. Volumetric model

Let us introduce the material removal rate (Q) [cm^3/min] and assume that, this quantity is proportion to the power required to cut (P):

$$P = Q \cdot K \text{ , [kW]} \tag{1}$$

where K constant depends on the workpiece material, cutting tool geometry and cutting conditions. The spindle motor power is equal to the tangential cutting force times the tooth velocity. Therefore, the tangential cutting force F_t is easily found by dividing the right side of (1) by the velocity. The radial force is calculated by multiplying the tangential force by a constant K_r:

$$F_t = \frac{Q \cdot K}{v_t} \quad , \quad F_r = K_r\, F_t \text{ . [N]} \tag{2}$$

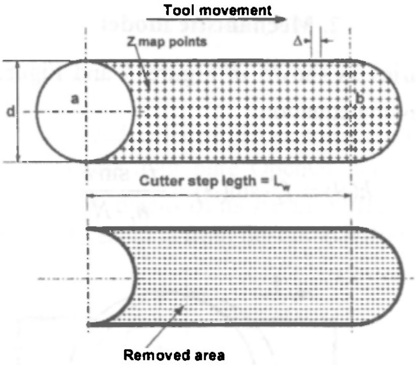

Fig. 1: Tool movement above dexel space

To determine this value for each tool movement we must calculate the volume removed: (see Figure 1)

$$V_m = \sum_{i=1}^{n_f} \left((z_2 - z_1)_i \cdot A_i \right) \qquad [\mathrm{cm}^3], \tag{3}$$

where A_i is the dexel area, z_2 and z_1 are the z values before and after the tool movement, n_f is the number of dexels modified by this particular tool movement:

$$Q = \frac{V_m}{time} = \frac{V_m}{\frac{L_w}{f}} \qquad [\mathrm{cm}^3/\mathrm{min}], \tag{4}$$

where f is the feedrate. The maximum possible error is easily calculated by looking at Figure 1. Unfortunately, this method is probably not useful for finishing. The basic shortcoming of this approach is that it only estimates average forces, not peak or instantaneous forces. (Fig 2)

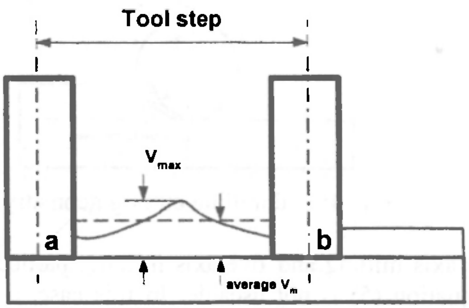

Fig. 2: Average removed volumes can be significantly different from the local maximum volume

2. Mechanistic model

The chip thickness $h(\vartheta)$ varies as shown in Figure 3 and Figure 4. For simple two axis cutting can be used the following equation:

$$h(\vartheta) = f_t \cdot \sin(\vartheta) = \frac{f \cdot \sin \vartheta}{n_t \cdot N} \qquad (5)$$

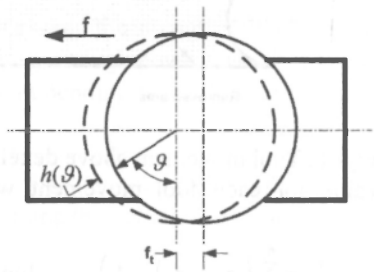

Fig. 3: Chip Thickness

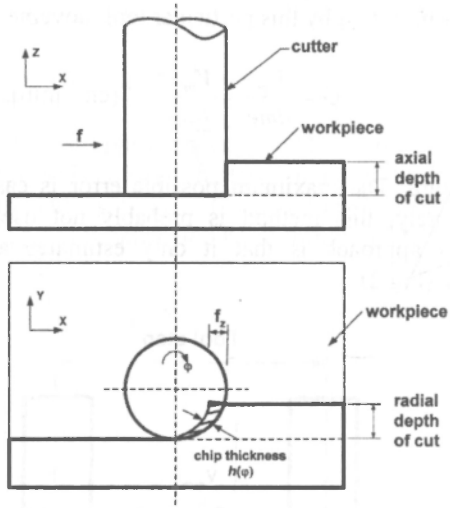

Fig. 4: End milling cutting geometry

In case of three axis milling and five-axis milling, particularly, if the cutting tool is ball-end mill, the equation (5) is not useable. In this case, a more complex equation is appropriate.

$$h(\vartheta,\varphi) = \frac{f(\vartheta,\varphi) \bullet N(\vartheta,\varphi)}{n_t \quad N}, \tag{6}$$

where the scalar product of the feed velocity $f(\varphi,z)$ and the cutting tool surface normal $N(\vartheta,z)$ determine the chip thickness. Our pure OpenGL based machining simulator can easily determine the contact-area by means of its stencil-buffer. The normal vectors can be coded as color values and easily rereadable from the color-buffer for further calculation.

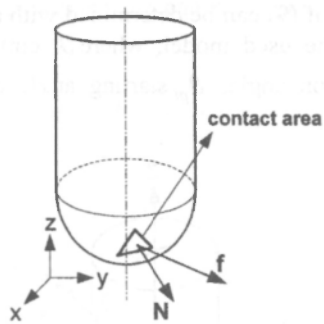

Fig. 5: Contact area on the ball-end cutter

2.2. Empirical cutting force model

Figure 6 shows a modell of the ball-end mill, where ϑ means the cutter rotation angle. There is a direct proportionality between chip thickness and cutting force. Tangential and radial components of the cutting force can be formulated as: [4]:

$$\begin{aligned} \Delta F_t &= K_t\, h(\varphi,z) \\ \Delta F_r &= K_r\, \Delta F_t\,. \end{aligned} \tag{7}$$

K_t and K_r depend on workpiece material and tool and cutting temperature and tool geometry. The force on the cutting edge depends on the cutter rotation angle and the helix angle. There are number of studies about the empirical evaluation of these constants [4-11]. In our special situation (7) can be expressed as:

$$\begin{aligned} dF_T &= K_T(\varphi)\, h(\vartheta,\varphi)^{m_T}\, dz \\ dF_R &= K_R(\varphi)\, h(\vartheta,\varphi)^{m_R}\, dz\,, \end{aligned} \tag{8}$$

where $0 < m_R < 1$ és $0 < m_T < 1$. K_T and K_R are function of φ angle. It is verifiable with lot of cutting test that $K_R(\varphi)$ has maximum at $\varphi = \frac{\pi}{4}$ and $K_T(\varphi)$ is a monoton function of φ. According to [5] these parameters we should approximate on the following way:

$$K_T(\varphi) = a_0 + a_1\varphi + a_2\varphi^2 + a_3\varphi^3$$
$$K_R(\varphi) = b_0 + b_1\varphi + b_2\varphi^2 + b_3\varphi^3 \tag{9}$$

These eight constant values of (9) can be determined with a lot of test cuts. Figure 7 shows the coordinate system of the used model, where ϑ cutter rotation angle, φ means the cutting edge element position angle, ϑ_{pi} starting angle of the helix, $\psi(\varphi)$ cutting edge position angle.

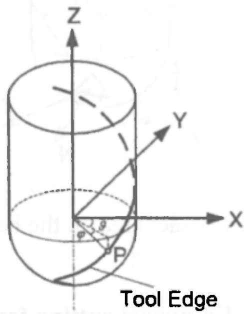

Fig. 6: Geometrical modell of a Ball-End cutter. An arbitrary element of the cutting edge can be experssed with φ, ϑ angles.

According to Figure 7, we can calculate the rotation angle of cutting edge element $\vartheta_i(\varphi)$ of th ith flute as follows [9]:

$$\vartheta_i(\vartheta,\varphi) = \vartheta + \vartheta_{pi} - \psi(\varphi) = \vartheta + (i-1)\frac{2\pi}{n} - \sin(\varphi)\tan(\beta), \tag{10}$$

where β is the helix angle, n is the number of flutes, i means the current flute. Let us substitute (10) into the equation of a helix and we will get:

$$x = R(\varphi)\cos\vartheta_i(\vartheta,\varphi)$$
$$y = R(\varphi)\sin\vartheta_i(\vartheta,\varphi), \tag{11}$$

where $R(\varphi) = \sqrt{R - (R - R\cos(\varphi))^2}$ on the sphere and $R(\varphi) = R$ on the cylinder part of cutting tool. We can easily represent (11) with Matlab software. (see: Fig 7) According to

Martelloti [11] the chip thickness can be approximate with (5) but Engin [9] recomended a more general formula:

$$h(\vartheta,\varphi) = f_z \sin\vartheta \sin\varphi\,. \tag{12}$$

In our model it is more natural to apply an other formula to calculate chip thickness as we have shown in equation (6).

If the rotating axis of the tool is non perpendicular to the feed direction (e.g.: real 3 axis machining) then XYZ coordinate system will rotate about X axis by ξ angle. (see: Fig 7) Differential height of the chip segment dz can be expressed with the diameter of the cutter and φ angle:

$$dz = R\cos\varphi\, d\varphi\,. \tag{13}$$

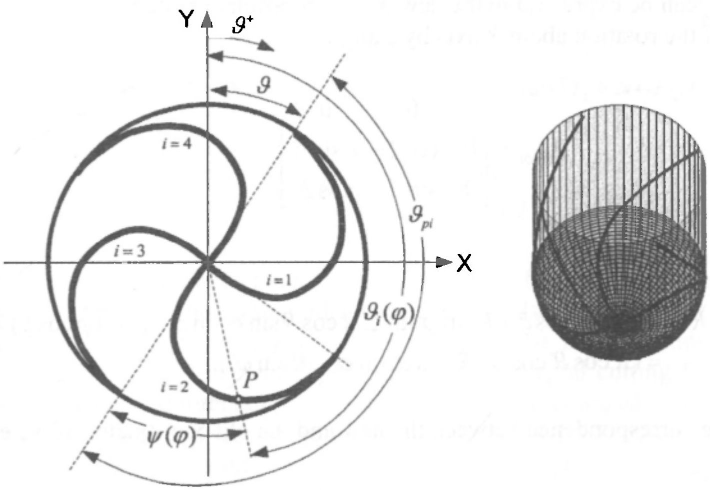

Fig. 7: Left side of the picture shows geometric model of the ball-end cutter on the right side can be seen MATLAB representation of (11).

The coordinates of cutting edge element P in the XYZ coordinate system:

$$P = (R\cos\vartheta\cos\varphi, R\cos\vartheta\sin\varphi, -R\sin\varphi)\,. \tag{14}$$

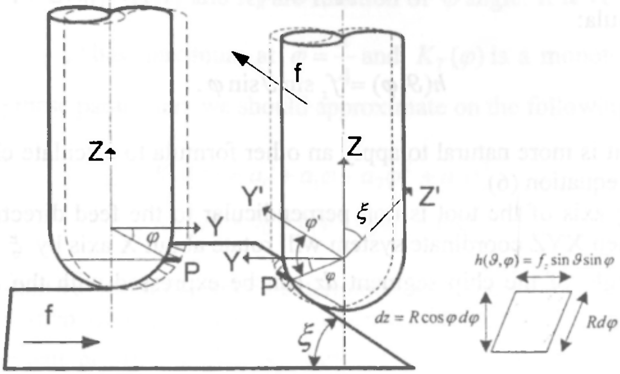

Fig. 8: In the case of upward/downward ramping the chip geometrycan be expressed in the new X'Y'Z' coordinate system

Matrix form of the rotation about X axis by ξ angle:

$$R_{Xrot} = \begin{bmatrix} 1 & 0 & 0 \\ 0 & \cos\xi & -\sin\xi \\ 0 & \sin\xi & \cos\xi \end{bmatrix} \tag{15}$$

P in XYZ coordinate system:

$$\begin{aligned} P = (R\cos\vartheta\cos\varphi, R\cos\vartheta\sin\varphi\cos\xi + R\sin\varphi\sin\xi. R\cos\vartheta\sin\varphi\sin\xi - R\sin\varphi\cos\xi) = \\ = (R\cos\vartheta'\cos\varphi', R\cos\vartheta'\sin\varphi', -R\sin\varphi'). \end{aligned} \tag{16}$$

We can find out the correspondence between the new and the old coordinates, if we express φ' and ϑ' from (16):

$$\varphi' = -\sin^{-1}(\cos\vartheta\sin\varphi\sin\zeta - \sin\varphi\cos\zeta), \tag{17}$$

$$\vartheta' = \cos^{-1}\left(\frac{\cos\vartheta\sin\varphi\cos\zeta - \sin\varphi\sin\zeta}{\sin\varphi'}\right). \tag{18}$$

Tangential and radial elemental forces can be calculated from (8) and (6):

$$\begin{aligned} dF_T &= K_T(\varphi)\left[f_z \bullet N(\vartheta(\vartheta,\varphi),\varphi)\right]^{m_T} R\cos\varphi' d\varphi' \\ dF_R &= K_R(\varphi)\left[f_z \bullet N(\vartheta(\vartheta,\varphi),\varphi)\right]^{m_R} R\cos\varphi' d\varphi'. \end{aligned} \tag{19}$$

dF_x and dF_y can be calculated with the following formula:

$$\begin{bmatrix} dF_X \\ dF_Y \\ dF_Z \end{bmatrix} = R_Z(\vartheta) \begin{bmatrix} dF_t \\ dF_r \\ dF_A \end{bmatrix}, \tag{20}$$

where:

$$R_Z(\vartheta) = -\begin{bmatrix} \cos\vartheta & \sin\vartheta & 0 \\ -\sin\vartheta & \cos\vartheta & 0 \\ 0 & 0 & 1 \end{bmatrix}. \tag{21}$$

Executing the operation in (20) and summarizing along the cutting edge:

$$F_x(\vartheta) = \int \rho R \{-K_T(\varphi) \left[f_z \bullet N(\vartheta(\vartheta,\varphi),\varphi)\right]^{m_T} \cos\vartheta - K_R(\varphi) \left[f_z \bullet N(\vartheta(\vartheta,\varphi),\varphi)\right]^{m_R} \sin\vartheta\} \cos\varphi' d\varphi'$$

$$F_y(\vartheta) = \int \rho R \left\{K_T(\varphi) \left[f_z \bullet N(\vartheta(\vartheta,\varphi),\varphi)\right]^{m_T} \sin\vartheta - K_R(\varphi) \left[f_z \bullet N(\vartheta'(\vartheta,\varphi),\varphi)\right]^{m_R} \cos\vartheta\right\} \cos\varphi' d\varphi'$$

$$\rho = \begin{cases} 1 & \textit{engaged} \\ 0 & \textit{not engaged} \end{cases} \tag{22}$$

The 3 dimensional contact area, which is obtained from the stencil buffer, is projected onto the cutter plane. The cutting edge elements are also projected onto the cutter plane. The cutting edge element engages in the cutting process if its position is on the contact area. If the cutting edge element engages then the elemental cutting forces are calculated from (8). By numerical integration instanteous cutting forces are calculated from (22).

In Figure 10, you can see a screen-shot of our pure OpenGL based milling simulator, in which we are planning to apply this new cutting force model.

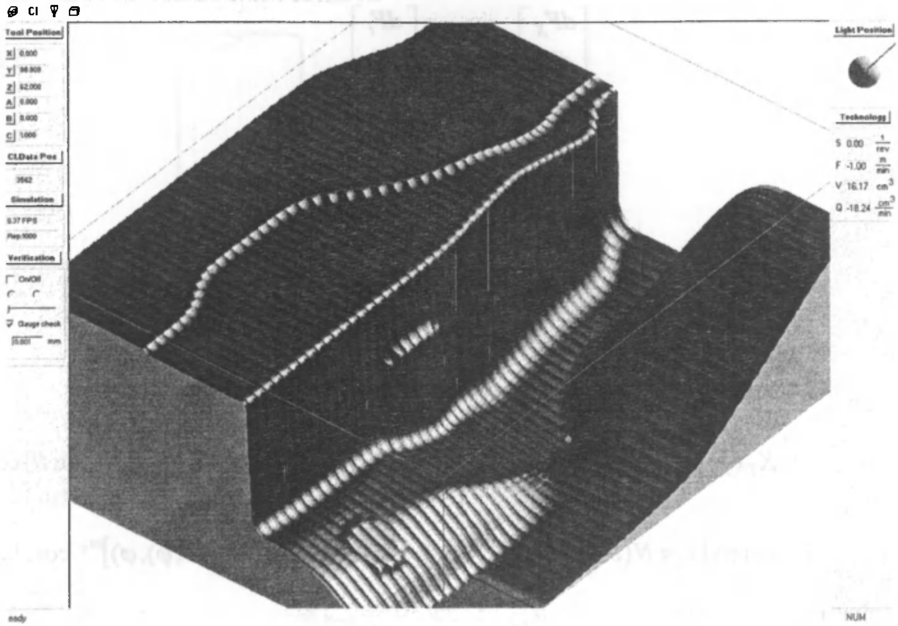

Fig. 9: Our pure OpenGL based milling simulator in which we are planning to apply this new cutting force model

4. Acknowledgements

The author is grateful to the colleagues of the Department of Information Engineering at University of Miskolc. Special thanks are due to Professor Tibor Tóth for his constructive comments and advice.

REFERENCES

NEHÉZ, K., VELEZDI, Gy., CSÁKI, T.: *Efficient Simulation of 3-5 Axis Milling*, MicroCAD International Conference 2001 Miskolc, Hungary.

2. CHOI, B., JERALD, R.: *Sculptured Surface Machining – Theory and Applications*, 1998, ISBN 0-412-78020-8, Kluwer Academic Publisher.

3. JERALD, B., FUSSEL, K., T.: *On-line Optimization of Cutting Conditions for NC Machining*, 2001 NSF Design, Manufacturing & Industrial Innovation Research Conference, Jan 7-10, Tampa, Florida.

4. LEE, P., ALINTAS, Y *Prediction of Ball-end Milling Forces from Orthogonal Cutting Data*, Int. J. Mach. Tools Manufacture, 1995,Vol. 36. No.9, pp. 1059-1072.

5. FENG, H.Y., MENQ, C. H.: *The Prediction of Cutting Forces in the Ball-End Milling Process-I Model Formulation and Model Building Procedure*, Int. J. Mach. Tools Manufacture, 1994, Vol. 34. No.5, pp. 697-710.

6. FENG, H. Y., MENQ, C. H.: *The Prediction of Cutting Forces in the Ball-End Milling Process-II. Cut Geometry Analysis and Modell Verification*, Int. J. Mach. Tools Manufacture, 1994, Vol. 34. No.5, pp. 711-719.

7. TAI, C. C., FUH, K. H.: *Model for Cutting Forces Prediction in Ball-End Milling*, Int. J. Mach. Tools Manufacture, 1994, Vol. 35. No.4, pp. 511-534.

8. LI, H.Z., LI, X.P.: *Milling Force Prediction Using a Dynamic Shear Length Model*, Int. J. Mach. Tools Manufacture, 2001, Vol. 42. pp. 277-286.

9. ENGIN, S., ALTINTAS, Y.: *Mechanics and Dynamics of General Milling Cutters. Part I: Helical End Mills*, Int. J. Mach. Tools Manufacture, 2001, Vol. 41. pp. 2195-2212.

10. ENGIN, S., ALTINTAS, Y.: *Mechanics and Dynamics of General Milling Cutters. Part II: Inserted cutters*, Int. J. Mach. Tools Manufacture, 2001, Vol. 41. pp. 2213-2231. 2001.

11. MARTELLOTI, M.E.: *An analysis of the milling process*, 1941, Trans. ASME 63 677-700.